

UV Laser Spectroscopy of Mass-Selected Ionic Liquid Building Blocks in the Gas-Phase

Contact Caroline.Dessent@york.ac.uk

A. J. A. Harvey

Department of Chemistry, University of York
Heslington
York
YO10 5DD, UK

A. Sen

Department of Chemistry, University of York
Heslington, York
YO10 5DD, UK

N. Yoshikawa

Department of Chemistry, University of York
Heslington, York
YO10 5DD, UK

C.E.H. Dessent

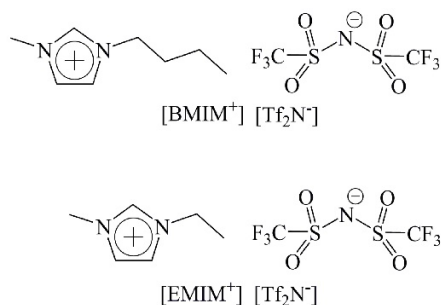
Department of Chemistry, University of York
Heslington, York
YO10 5DD, UK

This report is reproduced from the published article (with permission): *Chemical Physics Letter*, 634, 216-220, 2015.

Introduction

Ionic liquids have attracted considerable attention in both the fundamental and industrial chemical community over the last decade as a result of their unique physicochemical properties such as low vapour pressure, high viscosity and good conductivity. Proposed applications range from green industrial solvents, CO₂ extraction media, through to rocket propellants.¹⁻⁴ A very considerable number of spectroscopic studies have been conducted on condensed phase ionic liquids (ILs) with the aim of developing analytical methods for characterising ILs as well as to investigate their fundamental structure.^{5,6} Such work has been complemented by gas-phase studies of IL vapours over recent years, following the discovery that certain ILs were sufficiently volatile to allow transfer into the vapour phase within a high vacuum environment.^{7,8} These studies indicate that the IL vapours typically consist of ion-pairs for aprotic ILs,⁹⁻¹¹ and spectroscopic characterisation of such systems therefore provides an excellent opportunity for testing the large number of theoretical calculations that have been conducted on IL ion pairs.¹²⁻¹⁴

In this paper, we present UV laser photodissociation spectra of mass selected aggregate clusters of the [BMIM⁺][Tf₂N⁻] and [EMIM⁺][Tf₂N⁻] ILs, *i.e.* [BMIM⁺]_n[Tf₂N⁻]_m and [EMIM⁺]_n[Tf₂N⁻]_m where $n \neq m$ and $n, m = 1, 2$. Schematic structures of these ILs are displayed in Scheme 1.



Scheme 1: Structures of the a) [BMIM⁺][Tf₂N⁻] and b) [EMIM⁺][Tf₂N⁻] Ionic Liquids.

These spectra are the first such gas-phase UV spectra where the identity of the IL aggregate cluster can be definitively identified via mass selection prior to spectroscopic characterisation. Our general strategy mirrors that recently employed by Johnson and co-workers in their IR laser spectroscopy study of [EMIM⁺]_n[BF₄⁻]_m $n \neq m$ aggregate ions.¹⁵ We have chosen to study the [BMIM⁺][Tf₂N⁻] and [EMIM⁺][Tf₂N⁻] systems for this work as both have recently been the subject of vapour-phase UV spectroscopy studies,^{16,17} allowing us to address the key point of how closely the spectra of our mass-selected aggregates resemble those of the vapour-phase ILs. Wang *et al.* presented the first UV spectroscopic measurements of IL vapours (including the BMIM and EMIM systems) using high-temperature vaporization of ILs into quartz cuvettes,¹⁶ while Ogura *et al.* subsequently acquired a UV absorption spectrum of vapour phase [EMIM⁺][Tf₂N⁻] using cavity ring down spectroscopy.¹⁷ Cooper *et al.* have introduced [EMIM⁺][Tf₂N⁻] into the gas-phase in a supersonic expansion and applied UV photofragmentation to the resulting (non-mass selected) jet-cooled neutral clusters.¹⁸ In our current study, electrospray ionisation is used to transfer the ILs from the condensed phase into the gas-phase, prior to mass selection in a laser-interfaced mass spectrometer. We present electronic spectra of the anionic and cationic aggregates for both ILs for comparison with the previous gas-phase studies.

Experimental

Experiments were conducted in Bruker Esquire 6000 and Bruker AmaZon Quadrupole Ion Trap mass spectrometers that have been custom-modified for performing laser spectroscopy.^{19,20} The ILs were purchased from Aldrich and used without any further purification. IL clusters were generated using positive and negative mode electrospray (100°C dry gas temperature) ionization of 10⁻⁴ mol dm⁻³ (Esquire) and 10⁻⁶ mol dm⁻³ (AmaZon) solutions of the respective IL in acetonitrile, and specific mass-selected IL aggregates were isolated in the instrumental ion-trap and subjected to laser irradiation. UV photons were produced by an Nd:YAG (Continuum Surelite) pumped OPO (Panther), producing ~1.5mJ across 220-300 nm, and by an Nd:YAG (Continuum Powerlite) pumped Sirah PRSC dye laser (Coumarin 440 dye). 220 nm is the high-energy limit of this laser. Action spectra were recorded by monitoring the production of photofragments as a function of laser wavelength.²¹ All spectra are corrected for laser power. UV spectra of 0.1 mM [BMIM⁺][Tf₂N⁻] and [EMIM⁺][Tf₂N⁻] in acetonitrile were acquired with a Shimadzu UV-1800 spectrophotometer.

Results and Discussion

Figure 1a displays the positive ion mode electrospray ionisation mass spectrum (ESI-MS) obtained by electrospraying the $[\text{BMIM}^+][\text{Tf}_2\text{N}^-]$ IL in acetonitrile. The mass spectrum is dominated by the $[\text{BMIM}^+]_2[\text{Tf}_2\text{N}^-]$ aggregate cluster peak, with the $[\text{BMIM}^+]$ cation also clearly visible. Negatively charged aggregate clusters were observed when the instrument was operated in negative ion mode (Figure 1b), as illustrated by the strong appearance of $[\text{BMIM}^+][\text{Tf}_2\text{N}^-]_2$. Similar spectra were obtained in positive and negative ion mode when $[\text{EMIM}^+][\text{Tf}_2\text{N}^-]$ was electrosprayed in acetonitrile. The mass spectra obtained in this work resemble those observed in previous electrospray mass spectrometry studies of ILs.²²⁻²⁵ In this study we obtained spectra for the simplest aggregate clusters, *i.e.* the aggregates containing either two cations with an anion, $[\text{C}^+]_2[\text{A}^-]$, or two anions with a cation, $[\text{C}^+][\text{A}^-]_2$. Higher aggregate clusters are present in the ESI-MS, but with considerably lower intensities.

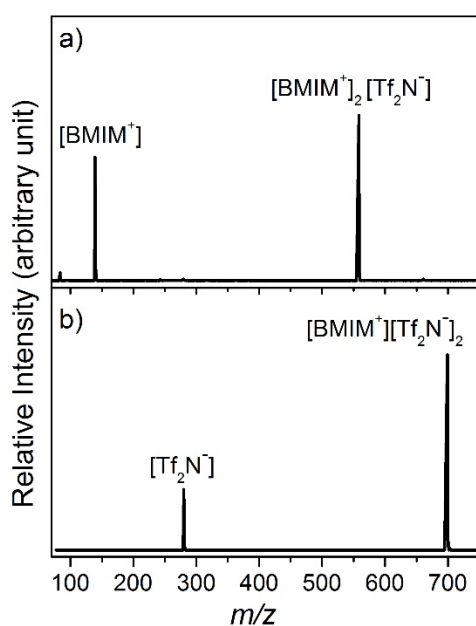
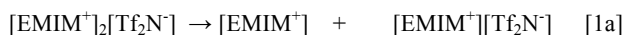
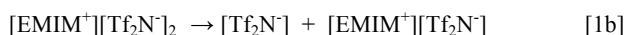


Figure 1: a) Positive ion mode ESI-MS of the $[\text{BMIM}^+][\text{Tf}_2\text{N}^-]$ ionic liquid in acetonitrile, and b) corresponding negative ion mode spectrum. The m/z values for the observed species are m/z $[\text{BMIM}^+] = 139$, m/z $[\text{BMIM}^+]_2[\text{Tf}_2\text{N}^-] = 558$, m/z $[\text{Tf}_2\text{N}^-] = 280$, and m/z $[\text{BMIM}^+][\text{Tf}_2\text{N}^-]_2 = 699$.

All of the spectra presented in this study are action spectra, and it is therefore necessary to identify the photofragment ions prior to conducting spectral scans. Figures 2a and 2b present the photofragmentation mass spectra obtained upon 220 nm excitation of the mass-selected $[\text{EMIM}^+]_2[\text{Tf}_2\text{N}^-]$ and $[\text{EMIM}^+][\text{Tf}_2\text{N}^-]_2$ from the $[\text{EMIM}^+][\text{Tf}_2\text{N}^-]$ IL. 220 nm is the high-energy limit of this laser. Figure 2a illustrates that the cationic $[\text{EMIM}^+]_2[\text{Tf}_2\text{N}^-]$ cluster photofragments with production of $[\text{EMIM}^+]$ as the sole ionic photofragment, presumably accompanied by loss of a neutral ion pair which is undetected in the mass spectrometer, *i.e.*



The anionic cluster $[\text{EMIM}^+][\text{Tf}_2\text{N}^-]_2$ similarly produces $[\text{Tf}_2\text{N}^-]$ as the sole ionic photofragment (Figure 2b), again presumably along with an accompanying neutral ion pair:



The cationic and anionic aggregates from $[\text{BMIM}^+][\text{Tf}_2\text{N}^-]$ (Figures 2c and 2d) were observed to photofragment in the same way as for $[\text{EMIM}^+][\text{Tf}_2\text{N}^-]$. We note that the photofragmentation pathways mirror the cluster fragmentation patterns observed upon collision induced dissociation of ground state IL aggregates, which fragment with loss of a neutral ion-pair unit.²⁵

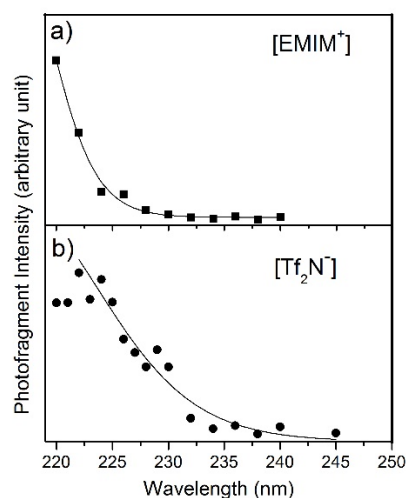


Figure 2: Photofragmentation mass spectra of a) $[\text{EMIM}^+]_2[\text{Tf}_2\text{N}^-]$, b) $[\text{EMIM}^+][\text{Tf}_2\text{N}^-]_2$, c) $[\text{BMIM}^+]_2[\text{Tf}_2\text{N}^-]$ and d) $[\text{BMIM}^+][\text{Tf}_2\text{N}^-]_2$ recorded at 220 nm. The m/z values for the observed species are m/z $[\text{EMIM}^+] = 111$, m/z $[\text{EMIM}^+]_2[\text{Tf}_2\text{N}^-] = 502$, m/z $[\text{Tf}_2\text{N}^-] = 280$, m/z $[\text{EMIM}^+][\text{Tf}_2\text{N}^-]_2 = 671$, m/z $[\text{BMIM}^+] = 139$, m/z $[\text{BMIM}^+]_2[\text{Tf}_2\text{N}^-] = 558$, m/z $[\text{Tf}_2\text{N}^-] = 280$, and m/z $[\text{BMIM}^+][\text{Tf}_2\text{N}^-]_2 = 699$.

Figure 3a displays the photofragment action spectrum for the $[\text{EMIM}^+]$ fragment from $[\text{EMIM}^+]_2[\text{Tf}_2\text{N}^-]$ across the spectral range from 220-245 nm. The maximum photofragment production over this range occurs at 220 nm, the high-energy limit for our laser system, with the photofragment intensity falling away very rapidly to longer wavelengths (effectively zero above 230 nm). Figure 3b shows the action spectrum for production of $[\text{Tf}_2\text{N}^-]$ from $[\text{EMIM}^+][\text{Tf}_2\text{N}^-]_2$, again displaying a maximum value at 220 nm, but with a slightly less sharp fall-off in intensity towards longer wavelength. The intensity of the anionic photofragment from excitation of the anionic aggregate was much smaller than that of the cationic fragment from photoexcitation of the cationic aggregate, with anion photofragment signals typically being on the order of 100 times smaller than the cation photofragment.

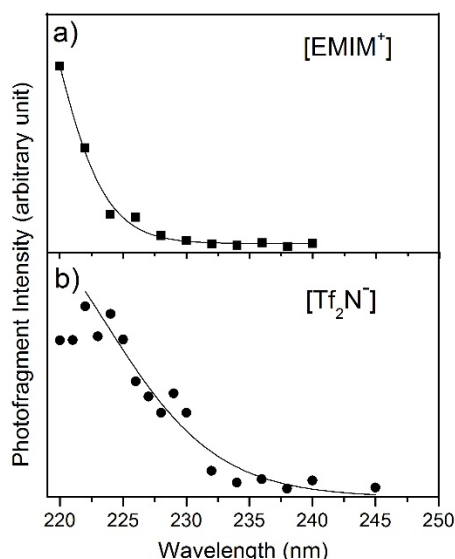


Figure 3: Cluster photofragment action spectra of a) $[\text{EMIM}^+]$ from the $[\text{EMIM}^+]_2[\text{Tf}_2\text{N}^-]$ cationic aggregate and b) $[\text{Tf}_2\text{N}^-]$ from the $[\text{EMIM}^+][\text{Tf}_2\text{N}^-]_2$ anionic aggregate.

The corresponding action spectra obtained for the $[\text{BMIM}^+][\text{Tf}_2\text{N}^-]$ IL aggregates (Figures 4a and 4b) are similar to those of $[\text{EMIM}^+][\text{Tf}_2\text{N}^-]$. The $[\text{BMIM}^+]$ fragment spectrum (Fig. 4a), is very similar to the corresponding $[\text{EMIM}^+]$ fragment spectrum (Fig. 3a), with the intensity falling away rapidly at wavelengths longer than 220 nm, while the decrease in the $[\text{Tf}_2\text{N}^-]$ fragment (Fig. 4b) from excitation of the $[\text{BMIM}^+][\text{Tf}_2\text{N}^-]_2$ anionic aggregate is more gradual. The intensity of the anionic photofragment was again significantly smaller than the cationic photofragment, as in the $[\text{BMIM}^+]_n[\text{Tf}_2\text{N}^-]_m$ aggregates.

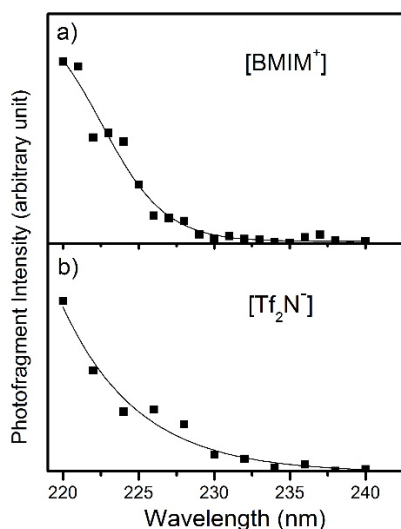


Figure 4: Cluster photofragment action spectra of a) $[\text{BMIM}^+]$ from the $[\text{BMIM}^+]_2[\text{Tf}_2\text{N}^-]$ cationic aggregate and b) $[\text{Tf}_2\text{N}^-]$ from the $[\text{BMIM}^+][\text{Tf}_2\text{N}^-]_2$ anionic aggregate.

Solution-phase UV spectra (Figure 5) were recorded for both $[\text{EMIM}^+][\text{Tf}_2\text{N}^-]$ and $[\text{BMIM}^+][\text{Tf}_2\text{N}^-]$ for comparison with the gas-phase action spectra. Each IL displays a strong UV band with an onset around 235 nm and absorption bands peaked around 220 nm ($\lambda_{\text{max}} = 211$ nm for $[\text{EMIM}^+][\text{Tf}_2\text{N}^-]$ and $\lambda_{\text{max}} = 210$ nm for $[\text{BMIM}^+][\text{Tf}_2\text{N}^-]$). This band is associated with excitation of the $\pi-\pi^*$ chromophore which exists in imidazole-type molecules in this region.²⁶

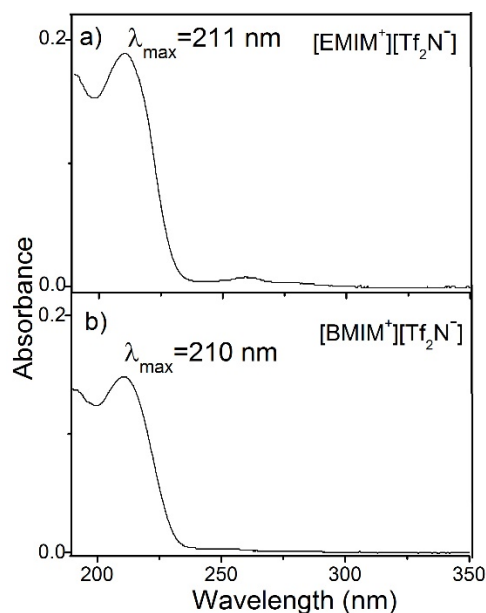


Figure 5: Liquid phase UV absorption spectra of a) $[\text{EMIM}^+][\text{Tf}_2\text{N}^-]$ and b) $[\text{BMIM}^+][\text{Tf}_2\text{N}^-]$.

Gas-phase spectroscopic studies of the isolated imidazole molecule have revealed the presence of a bright optical excited state that is coupled to a dark dissociative state, resulting in a broad absorption band.^{27,28} Although our photofragment spectra display maximum values at 220 nm, we are currently unable to assign λ_{max} values for the gas-phase aggregate clusters due to the limitations of our laser system. Figure S1 presents a second set of photofragmentation action spectra for the $[\text{EMIM}^+][\text{Tf}_2\text{N}^-]$ aggregates, which have been recorded up to 215 nm with an additional laser system that provided photons deeper into the UV. The photofragment intensity is still increasing at 215 nm, indicating that λ_{max} occurs at shorter wavelengths.

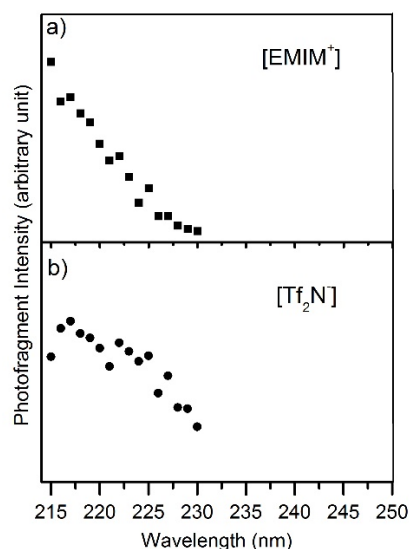


Figure S1: Cluster photofragment action spectra of a) $[\text{EMIM}^+]$ from the $[\text{EMIM}^+]_2[\text{Tf}_2\text{N}^-]$ cationic aggregate and b) $[\text{Tf}_2\text{N}^-]$ from the $[\text{EMIM}^+][\text{Tf}_2\text{N}^-]_2$ anionic aggregate. These spectra were recorded with an Nd:YAG pumped OPO system that provided photons to 215 nm at the high energy limit. The spectra display similar profiles to the spectra presented in Figure 3 of the main manuscript, with an additional scanned range from 220-215 nm.

The photofragment action spectrum for the IL aggregates displayed in Figures 3 and 4 display similar absorption profiles

to the UV absorption spectra of these ILs recorded by Wang et al. for the IL vapour (557 K) contained in a quartz cuvette, i.e. broad onset above 240 nm with rising absorbance towards 200 nm.¹⁶ Wang et al. recorded spectra at temperatures from 533-573 K, showing that the absorption onset is displaced to longer wavelength at higher temperature. The redder onset absorptions seen in the high-temperature vapour spectra are likely due to higher-energy conformations (of IL ion-pairs), as well as rotational and vibrational excitation. The ESI aggregates studied in our experiment are thought to have temperatures of ~373K,¹⁹ hence explaining the comparatively blue-shifted absorbance onsets. Our [BMIM⁺][Tf₂N⁻] photofragment action spectra are also very similar to those obtained for this IL by Ogura et al. using single-path absorption and cavity ring-down absorption spectroscopy.¹⁷ The spectra of Ogura *et al.* were obtained at temperatures (406-429 K) much closer to the temperature of our aggregates, and hence display absorption onsets (~233 nm at 418 K) closer to our value (230 nm). Finally, it is of interest to compare our [EMIM⁺]_n[Tf₂N⁻]_m aggregate data to the spectra recorded by Cooper et al. in their photodissociation study of the IL [EMIM⁺][Tf₂N⁻] in a supersonic expansion.¹⁸ Figure S2 displays our [EMIM⁺][Tf₂N⁻] data in the same form as the Cooper et al. data allowing a direct comparison. Again, our data are very similar to the Cooper et al. results. The overall picture to emerge from these spectroscopic comparisons is that the mass-selected aggregates studied in this work appear to behave as simple ion-pairs, with the excess charged unit (*i.e.* [EMIM⁺] in the cationic cluster and [Tf₂N⁻] in the anionic cluster of the [EMIM⁺]_n[Tf₂N⁻]_m aggregates) only weakly perturbing the photoexcitation and photodissociation dynamics.

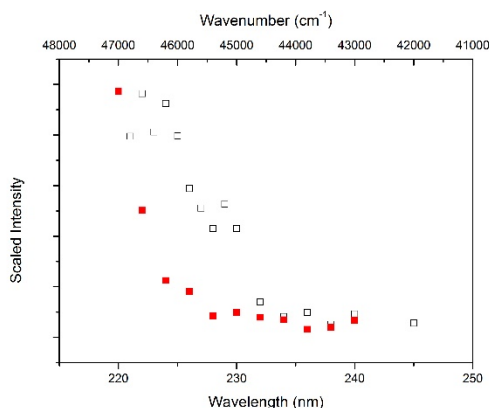


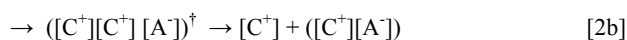
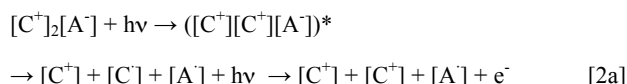
Figure S2: Overlay of the cation (closed squares) and anion (open squares) photofragment action spectra from the cationic and anionic aggregates of [EMIM⁺][Tf₂N⁻]. The anion and cation signals are scaled to be shown with the same intensity for the maximum points.

Further Discussion

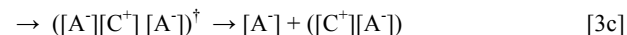
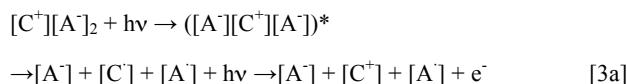
The similarity between the [EMIM⁺]_n[Tf₂N⁻]_m aggregate photofragment spectra observed in this work, and the [EMIM⁺][Tf₂N⁻] supersonic jet spectra measured by Cooper et al. suggest that similar photophysics may be present in photoexcitation of the aggregates as in the isolated ion-pairs that are thought to be present in the jet experiment. Cooper et al. have proposed a mechanism that involves initial photoexcitation to an electronic excited state of the [EMIM⁺][Tf₂N⁻] ion-pair.¹⁸ They postulate that the major pathway for decay of the excited state is predissociation by a charge-transfer state as seen by Leone and co-workers,²⁹ resulting in production of the [EMIM][Tf₂N] radical pair, where the reduced cation moiety can then be ionized by a

second photon to produce [EMIM⁺]. Thus, the dominant ionic photofragment is [EMIM⁺], produced in a two-photon process. In addition, they suggest that a much more minor pathway exists corresponding to direct decay of the excited state back to the ground electronic state, from where ergodic dissociation occurs producing [EMIM⁺] and [Tf₂N⁻] as minor ionic photofragment products.

The strong production of the cationic photofragments and comparatively weak production of the anionic photofragments observed following excitation of the IL aggregates in this work mirrors the observations of Cooper et al. and suggests that a similar mechanism may be operating. For the cationic aggregates, [C⁺]₂[A⁻], we propose that the mechanism of Cooper et al. would be modified as follows:



where [2a] corresponds to the dominant predissociation pathway followed by C⁺ ionization (IE_C is thought to be ~3.9 eV for [EMIM⁺]¹⁸) while [2b] is the minor excited-state to ground-state decay route. (Note that the thermally excited ground-state cluster, ([C⁺][C⁺][A⁻])[†], will decay with loss of a neutral ion-pair unit as observed for collision induced dissociation of the ground state clusters.²⁵) Overall, the combined [2a]+[2b] pathways would lead to strong production of the [C⁺] ion, consistent with the experimental observation. We note that no anionic photofragment is produced in either step [2a] or [2b], but we are unable to test this in our experimental set-up as only cationic photofragments can be detected after isolating a cationic precursor. The analogous pathways for the anionic aggregates would be:



where [3a] and [3b] correspond to the dominant predissociation followed by either C⁺ ionization or [A⁻] photodetachment (the detachment energy of Tf₂N⁻ is calculated to be around 5.6 eV at the M06/6-311++G** level),¹⁸ whereas [3c] is a minor pathway that results in [A⁻] as the sole ionic photofragment. This photofragment would again be susceptible to photodetachment through interaction with a third photon during the time the ions are stored in the ion trap. It is clear that [A⁻] is only likely to be observed as a weak photoproduct from the combined series of [3a]→[3c] pathways.

Cooper et al. have performed power dependent measurements to support their proposed mechanism, but such definitive measurements that unambiguously determine the number of photons involved in production of each photofragment have not been performed in the ion trap instrument used in this study, since precursor ions and photofragment ions may undergo multiple interactions with different photons over the timescale that ions are stored in the trap. Nonetheless, preliminary measurements of photofragment intensity versus laser power for the [BMIM⁺]_n[Tf₂N⁻]_m aggregates clearly revealed that the power dependence for production of the cationic photofragments is different from the anionic photofragments, consistent with distinctive fragmentation pathways.

Summary

Since the chemical and physical properties of ILs can be controlled by the combination of cationic and anionic components, ILs can be used for an increasingly wide range of technical applications.¹⁻⁴ Given the wealth of possible cation-anion combinations, it is highly desirable to be able to rationally predict the properties of an IL based on the constituents.³⁰ Ab initio computational studies of ILs make a considerable contribution to this general effort, but such calculations are typically performed on isolated “gas-phase” systems.¹²⁻¹⁴ It is therefore important to be able to study IL building blocks (i.e. ion-pairs or aggregates) in the gas-phase. While IR vibrational spectroscopy of gas-phase ILs focus on characterising geometric structures, studies of the electronic spectroscopy of gaseous ILs are also of crucial importance for determining the intrinsic absorption and fluorescence behaviour of ILs both to clarify liquid-phase anomalies (e.g. additional charge transfer bands, contributions from clusters, and charge transfer to solvent bands in mixed media),^{17,31,32} and also to provide benchmark data for TD-DFT and other excited state calculations.³⁰

The experiments performed in this work demonstrate the feasibility of exploring the excited state photophysics of ILs via the study of mass-selected charged aggregates produced via electrospray ionisation. The UV gas-phase absorption profiles measured in this way show that this technique provides a facile route to obtaining gas-phase UV spectra of ILs. One considerable advantage of our technique over the previous methods is that there is no contamination of our spectra from impurities due to the mass-selection employed prior to laser excitation. Indeed, the presence of impurities in IL samples can be substantial,³³ and considerable effort needs to be expended to ensure that samples are pure prior to routine spectroscopic analysis.

Numerous further experiments are possible from these initial spectroscopic measurements, and it will be valuable to move to cationic units that lack the dissociative excited state, and also to explore anionic units that possess a chromophore. Further theoretical work is also certainly desirable to more accurately characterise the rich photophysics evident in these mixed charge gas-phase clusters, both as a basis for understanding the fundamental photophysics of other novel mixed charge systems but also to inform our understanding of UV processes in bulk ILs.^{31,32}

Acknowledgements

This work was supported through the European Research Council grant 208589-BIOIONS. The Bruker Esquire 6000 was provided by Science City York and Yorkshire Forward using funds from the Northern Way Initiative. We also thank the STFC for the provision of equipment from the EPSRC Laser Loan Pool (Grant # 13250030).

References

1. N. V. Plechkova, K. R. Seddon, *Chem. Soc. Rev.* 37, 123 (2008).
2. J. P. Hallett and T. Welton, *Chem. Rev.* 111, 3508 (2011).
3. D. M. D'Alessandro, B. Smit, J. R. Long, *Angew. Chem. Int. Ed.* 49, 6058 (2010).
4. Y. Zhang, H. Gao, Y. H. Joo, J. M. Shreeve, *Angew. Chem. Int. Ed.* 50, 9554 (2011).

5. *Ionic Liquids (Topics in Current Chemistry)*, Barbara Kirchner, Springer, (2013).
6. *The Structure of Ionic Liquids (Soft and Biological Matter)*, R. Caminiti and L. Gontrani, Springer, (2013).
7. L. P. N. Rebelo, J. N. C. Lopes, J. M. S. S. Esperança, E. Filipe, *J. Phys. Chem. B*, 109, 6040 (2005).
8. M. J. Earle, J. M. S. S. Esperança, M. A. Gilea, J. N. C. Lopes, L. P. N. Rebelo, J. W. Magee, K. R. Seddon and J. A. Widegren, *Nature*, 439, 831 (2006).
9. A. Deyko, K. R. J. Lovelock, P. Licence and R. G. Jones, *Phys. Chem. Chem. Phys.*, 13, 16841 (2011).
10. K. Dong, L. Zhao, Q. Wang, Y. Song, S. Zhang, *Phys. Chem. Chem. Phys.*, 15, 6034 (2013).
11. J. P. Leal, J. M. S. S. Esperança, M. E. Minas da Piedade, J. N. C. Lopes, L. P. N. Rebelo and K. R. Seddon, *J. Phys. Chem. A*, 111, 6176 (2007).
12. T. Cremer, C. Kolbeck, K. R. J. Lovelock, N. Paape, R. Wölfel, P. S. Schulz, P. Wasserscheid, H. Weber, J. Thar, B. Kirchner, F. Maier, H.-P. Steinrück, *Chem. Eur. J.*, 16, 9018 (2010).
13. S. A. Katsyuba, E. E. Zvereva, A. Vidiš, P. J. Dyson, *J. Phys. Chem. A*, 111, 352 (2006).
14. P.A. Hunt, C. R. Ashworth, R. P. Matthews, *Chem. Soc. Rev.*, 44, 1257 (2015).
15. C. J. Johnson, J. A. Fournier, C. T. Wolke, M. A. Johnson, *J. Chem. Phys.*, 139, 224305 (2013).
16. C. Wang, H. Luo, H. Li, and S. Dai, *Phys. Chem. Chem. Phys.*, 12, 7246 (2010).
17. T. Ogura, N. Akai, A. Kawai, K. Shibuya, *Chem. Phys. Lett.*, 555, 110 (2013).
18. R. Cooper, A. M. Zolot, J. A. Boatz, D. P. Sporleder, and J. A. Stearns, *J. Phys. Chem. A*, 117, 12419 (2013).
19. A. Sen, T. F. M. Luxford, N. Yoshikawa, C. E. H. Dessent, *Phys. Chem. Chem. Phys.*, 16, 15490 (2014).
20. A. Sen, C. E. H. Dessent, *J. Phys. Chem. Lett.*, 5, 3281 (2014).
21. C.E.H. Dessent, J. Kim, M. A. Johnson, *Acc. Chem. Res.*, 31, 527 (1998).
22. Z. B. Alfassi, R. E. Huie, B. L. Milman, P. Neta, *Anal. Bioanal. Chem.*, 377, 159 (2003).
23. F. C. Gozzo, L. S. Santos, R. Augusti, C. S. Consorti, J. Dupont, M. N. Eberlin, *Chem. Eur. J.*, 10, 6187 (2004).
24. I. Nakurte, P. Mekss, K. Klavins, A. Zicmanis, G. Vavilina, S. Dubrovina, *Eur. J. Mass Spectr.*, 15, 471 (2009).
25. A. M. Fernandes, M. A. A. Rocha, M. G. Freire, I. M. Marrucho, J. A. P. Coutinho, L. M. N. B. F. Santos, *J. Phys. Chem. B*, 115, 4033 (2011).
26. A. Bolovinos, P. Tsekeris, J. Philis, E. Pantos, G. Andritsopoulos, *J. Mol. Spectrosc.*, 103, 240 (1984).
27. A. L. Devine, B. Cronin, M. G. D. Nix, M. N. R. Ashfold, *J. Chem. Phys.*, 125, 184302 (2006).
28. M. Barbatti, H. Lischka, S. Salzmann, C. M. Marian, *J. Chem. Phys.*, 130, 034305 (2009).
29. C. J. Koh, S. R. Leone, *Mol. Phys.*, 110, 1705 (2012).
30. H. Niedermeyer, C. Ashworth, A. Brandt, T. Welton, P.A. Hunt, *Phys. Chem. Chem. Phys.* 15, 11566 (2013).
31. A. Paul, A. Samanta, *J. Chem. Sci.* 118, 335 (2006).
32. A. Paul, P.K. Mandal, A. Samanta, *Chem. Phys. Lett.* 402, 375 (2005).
33. P. Nockemann, K. Binnemans, K. Driesen, *Chem. Phys. Lett.*, 415, 131 (2005).